INDONESIAN JOURNAL ON GEOSCIENCE
Geological Agency
Ministry of Energy and Mineral Resources

Journal homepage: http://ijog.geologi.esdm.go.id
ISSN 2355-9314, e-ISSN 2355-9306

Komatiitic Lamprophyre in West Sulawesi: First Evidence for >1350°C and 3.5 - 3.8 GPa Mantle Melts

Shaban Godang[1], Fadlin[2,3], Bambang Priadi[4], Arifudin Idrus[5], and I Gde Sukadana[5,6]

[1]Geochemistry, Rare Minerals, and REE Researcher
[2]Geological Engineering, Jenderal Soedirman University (UNSOED);
[3]Akita University (Japan)
[4]Department of Geology, Institute of Technology Bandung (ITB)
[5]Department of Geological Engineering, Gadjah Mada University (UGM)
[6]Centre for Nuclear Mineral Technology, National Nuclear Energy Agency (BATAN)

Corresponding authors: bpriadi@gl.itb.ac.id; godang.sc@gmail.com
Manuscript received: June, 25, 2018; revised: October, 16, 2019;
approved: April, 27, 2020; available online: February, 09, 2021

Abstract - The presence of lamprophyric lavas of Late Cenozoic in Talaya Volcanic Formation at the boundary between the subregencies of Mamuju and Tabulahan (Western Sulawesi) associated with the mantle enrichment rocks of the Adang Volcanics is the subject of this study. Petrologically, lamprophyre is composed of orthopyroxene (enstatite), clinopyroxene (augite), biotite, leucite, amphibole, magnetite, and autometasomatism of chlorite in grain minerals and groundmass. The lamprophyre is classified into monchiquite shoshonitic lamprophyre, and it has a komatiitic composition with the ratio of $MgO/Al_2O_3 > 0.7906$ (in wt %). The komatiitic monchiquite lamprophyre is characterized by high MgO (10.02 - 12.67 %), relatively low alumina (Al_2O_3= 10.98 - 11.70 %), SiO_2= 46.43 - 47.8 %, TiO_2 (0.84 - 1.00 %), FeOt (7.75 - 7.88 %), and relatively high content of alkaline (Na_2O: 2.20 - 2.59 %; K_2O: 1.58 - 2.45 %; Total alkali: 4.00 - 4.89 %, and CaO (9.29 - 10.71 %). The geochemical trace element plots using various diagrams suggests the geotectonic setting of the lamprophyric rock was formed in suprasubduction alkaline continental-arc, and the proposed source of magmatism comes from the suprasubduction activities from the east. The protolith of magma was originated from partial melting of depleted MORB mantle (DMM), composed of pyroxene-peridotite (garnet-lherzolite). The partial melting conditions are suggested to occur at high pressure (3.5 - 3.8 GPa) and the depth of ~120 km with melting temperature of >1350°C, and the magma is dominantly controlled by olivine fractional crystallization.

Keywords: komatiitic lamprophyre, mantle melts, soshhonitic, suprasubduction alkaline-arc

How to cite this article:
Godang, S., Fadlin, Priadi, B., Idrus, A., and Sukadana I.G., 2021. Komatiitic Lamprophyre in West Sulawesi: First Evidence for >1,350°C and 3.5 - 3.8 GPa Mantle Melts. *Indonesian Journal on Geoscience*, 8 (1), p.39-58. DOI: 10.17014/ijog.8.1.39-58

Introduction

Komatiite is a type of ultramafic mantle-derived volcanic rock with high magnesium, which contains more than 18 % MgO, and the spinifex texture or a variety of needle-like texture (Arndt and Nisbet, 1982; Dostal, 2008); whereas the komatiitic is representative of high-Mg with the ratio of MgO/Al_2O_3 above 0.7906 (in wt. %) (Jensen, 1976). The komatiitic magma is probably produced in very hot mantle upwellings or plumes (Schmeling and Arndt, 2017).

Lamprophyres are mesocratic to melanocratic igneous rocks, usually hypabyssal, with a panidiomorphic texture and abundant mafic phenocrysts of dark mica (biotite or Fe-phlogopite) and/or amphibole, with or without pyroxene, with or without olivine, and sometimes melilite and/or feldspathoid, set in a groundmass of the same minerals. Any feldspar, usually alkali feldspar, is restricted to the groundmass (Gillespie and Styles, 1999). The lamprophyres are known as exotic rocks, because they are difficult to classify unambiguously using the existing criteria. They are not amenable to classification according to modal proportions, such as the QAPF system, nor compositional discrimination diagrams, such as TAS (Le Maitre *et al*., 1989). It seems unlikely that a simple taxonomic system will be found unless the appropriate genetic criteria are applied, that is, unless the classification takes into account the genesis of the rocks (Woolley *et al*., 1996). Furthermore, lamprophyres are a complex group of rocks that have mineralogical similarities to some kimberlites and lamproites which are grouped into lamprophyric rocks (Rock, 1991). The classification of lamprophyric rocks is figured in the hierarchical chart below (Figure 1). The discrimination for lamprophyres, lamproites, and kimberlites is usually released by using the geochemical plotting on ternary diagram as proposed by Bergman, 1987.

The lamprophyric rocks primarily occur as dikes, lopoliths, laccoliths, stocks, and small intrusions. On a purely chemical basis, an extrusive lamprophyre (e.g. minette or monchiquite) might be classified as potassic trachybasalt, shoshonite, or latite using the total alkali-silica diagram (see TAS classification), or as absarokite, shoshonite, or banakite using a classification sometimes applied to potassium-rich lavas. Such chemical classifications ignore the distinctive textures and mineralogies of lamprophyres.

Potassium-rich rocks have intensively been studied for the purpose of understanding not only the differences between ultrapotassic magmas ($K_2O/Na_2O>2.0$), potassic ($1.52<K_2O/Na_2O<2.0$), transition alkaline from shoshonitic to potassic ($1.24<K_2O/Na_2O<1.52$), shoshonitic ($0.5<K_2O/Na_2O<1.24$), and sodic magmas ($K_2O/Na_2O<0.5$)(Turner *et al*., 1996; Godang *et al*., 2016), but also those between various types of K-rich lavas from different tectonic settings (e.g. Bergman, 1987; Foley *et al*., 1987; Muller *et al*., 1992). Therefore, the petrogenesis either of orogenic or anorogenic potassic lavas has been a subject of high interest, because they are commonly emplaced in an environment with complex

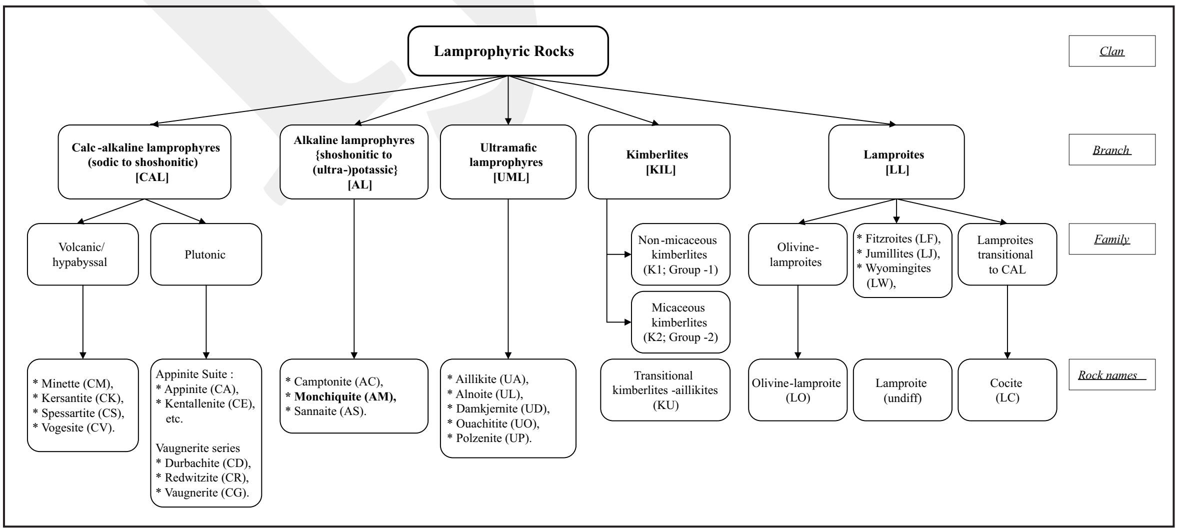

Figure 1. Hierarchical classification of lamprophyric rocks (adopted from Rock, 1991).

tectonic histories, which would facilitate better understanding and evaluating the role of various geological processes considered responsible for the origin of enrichment in potassium (and other highly incompatible elements) of K-rich magmas. These processes include the differentiation of primitive magma, fractionation of Mg to Fe in olivine and pyroxene, fractionation of crystalline minerals (such as fractionation of K-feldspar mineral from plagioclase), sediment subduction, crustal contamination, melt/fluid-related metasomatism, involvement of continental lithospheric mantle or asthenospheric mantle (e.g. Jensen, 1976; Schilling *et al.*, 1983; Varne, 1985; Rogers *et al.*, 1987; Foley, 1992a,b; Edwards *et al.*, 1994; Luhr, 1997; La Fleche *et al.*, 1998; Peccerillo, 1999; Carlson and Nowell, 2001; Abdel-rahman, 2002).

Large parts of the West Sulawesi Province are covered by thick (up to 5,000 m) piles of Upper Cenozoic shoshonitic to ultrapotassic and subordinate sodic volcanic rocks together with associated intrusive and volcaniclastics. The volcanic rocks occurring in the central part of the province have been subdivided into four units: Sekala Formation, and Sesean, Adang, and Talaya Volcanics (Ratman and Atmawinata, 1993) (Figure 2). The tectonic setting of Adang

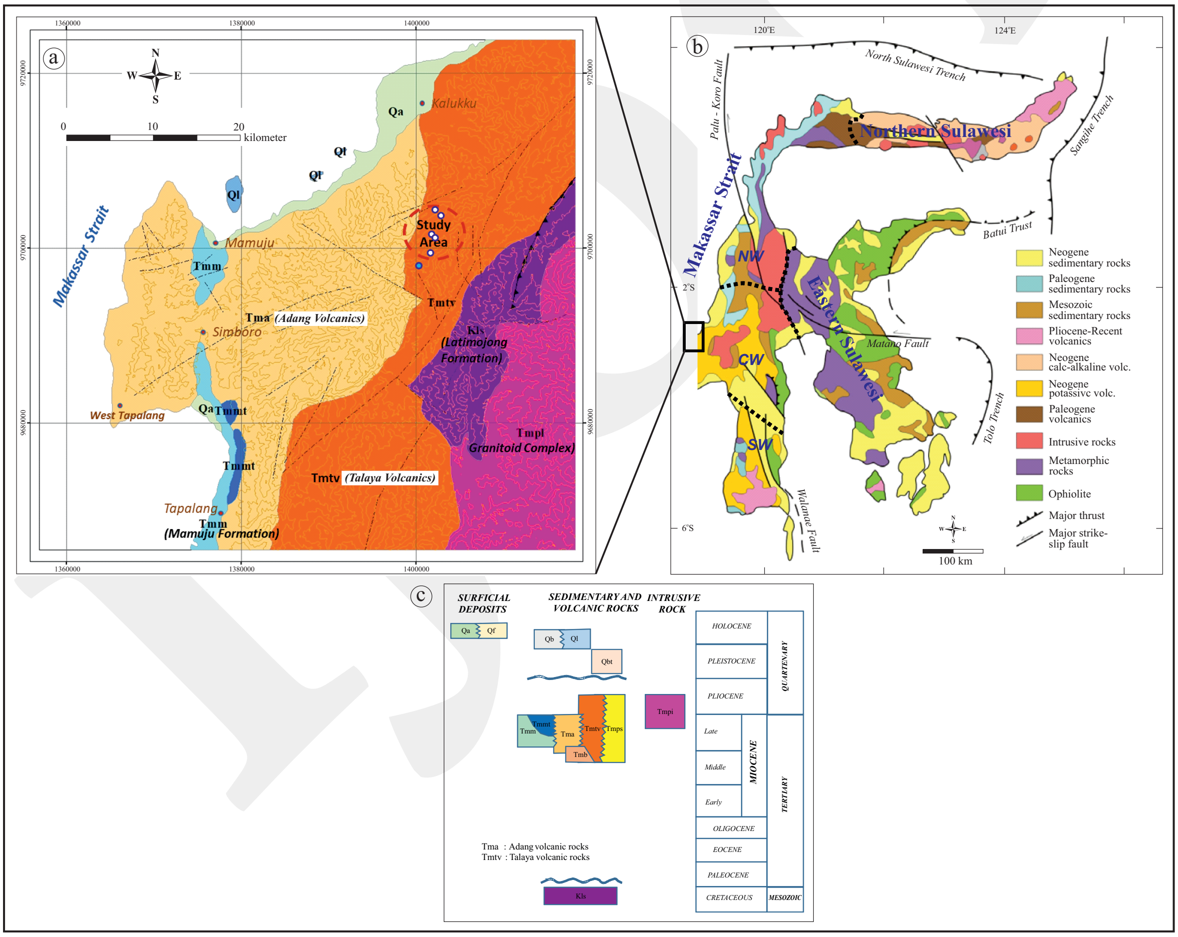

Figure 2. (a). Geological map of central Western Sulawesi (Ratman and Atmawinata, 1993) showing the location of study area. The coordinates of geological map use UTM zone 50S. The white circles are high-Mg lamprophyre sampling point, the blue circle is the other Adang Volcanic peralkaline dyke which exposed in the Talaya Volcanics. (b). Simplified geological map of Sulawesi {modified after Sukamto, 1975b; Hamilton, 1979; Silver *et al.*, 1983; Parkinson, 1991, (in Van Leeuwen and Pieters, 2011)}. Western Sulawesi (dashed line) subdivided into NW (Northwest; northern part of Western Sulawesi), CW (central-west) and SW (southwest) Sulawesi. (c). Correlation unit of Talaya Volcanics and Adang Volcanics. Talaya Volcanic rocks (Tmtv) were formed in Late Miocene to Pliocene, and Adang Volcanic rocks (Tma) formed in Mid to Late Miocene. In the researched zone, wherein of Talaya Volcanics oppresses the Adang Volcanics.

Volcanics were formed in a postsubduction, within-plate continental extension/initial rift tectonic setting, which consist of (ultra-) potassic to sodic series and were generated by minor (< 0.1 %) partial melting of depleted MORB mantle (DMM) material (garnet-lherzolite) with the silicate melt having undergone strong metasomatism (Godang *et al*., 2016). The magmatic process is also influenced by the continental crust component (Sukadana *et al*., 2015), whereas the tectonic of Talaya Volcanics has yet to be studied in detail. In general, the Talaya Volcanics is composed of andesitic-basaltic volcanic breccia, tuff and lava, with intercalation of sandstone and marl, local coal (Ratman and Atmawinata, 1993); whereas the Adang Volcanics is predominantly composed of leucite/pseudoleucite-bearing trachytic tuff, lapilli-tuff, agglomerate, volcanic breccia, volcanic-sedimentary products (volcaniclastics consisting of trachytic weathering residue, trachytic fragments), volcaniclastics and lava intercalations of basalt/basaltic to intermediate composition (consisting of leucite/pseudoleucite, diopside/aegirine and high temperature phlogopite) (Godang *et al*., 2016). In the research zone, Talaya Volcanics oppresses the Adang Volcanics, wherein the peralkaline dyke of Adang Volcanics and high-Mg lamprophyre lava were found in Talaya Volcanics. The presence of high-Mg lamprophyric lava in Talaya Unit which associated with the mantle enrichment rocks of the Adang Volcanics is a subject to be studied.

The aim of this study is to understand the genesis, geotectonic, and the melting conditions of high-Mg lamprophyre. The studied area is located at the boundary between Subregencies of Mamuju (Mamuju Regency) and Tabulahan (Mamasa Regency), West Sulawesi.

Materials And Methods

Geochemical analyses of major oxides, trace elements, and fifteen REE elements were carried out at Intertek Laboratories in Jakarta on July 2012 and August 2016, by using XRF (X-ray fluorescence), and ICP-MS (Inductively Coupled Plasma Emission Mass Spectrometry) with four acid digestions. Petrographic analysis was conducted at Mineral Resources Laboratory (Gadjah Mada University) on August 2016.

Results of Analyses

Field Observation and Petrography of Lamprophyre Rock

The field observations of lamprophyric lava show needle-like texture with pyroxene phenocryst and homogeneous chemical compositions (Figures 3). Petrologically, lamprophyre consists of 45 % of grain minerals with crystal (0.5 - 2.1 mm) such as orthopyroxene (enstatite, 2 %), clinopyroxene (augite, 25 %), biotite (8 %), leucite (10%), and amphibole (5 %) (Table 1);

Figure 3. Field observation photos of komatiitic lamprophyre in Talaya Volcanics. (a) The outcrop of lamprophyre at the streamlet, (b) The rock sample shows needle-like texture, the measurement of pyroxene phenocryst by ruler scale (~ 9mm), (c) Other Adang Volcanic peralkaline dyke in Talaya Volcanics.

Table 1. Results of Petrological Analysis of Komatiitic Lamprophyric Samples (vol.%)

Code#	#1
Location	
Rock names	
Sample_code	**#A01_2012**
Orthopyroxene (Enstalite)	2.00
Clinopyroxene (Augite)	25.00
Biotite	8.00
Leucite	10.00
Magnetite	2.00
Chlorite	10.00

whereas groundmass (40 %) with crystal size < 0.1 mm is composed of magnetite (2 %), auto-metasomatism of chlorite (10 %), lithic (xenolith; 5 %) of phonolitic leucitites with the dominant composition of leucite-clinopyroxene (Figure 4). According to Rock (1991), the lamprophyre containing 10% of chlorite was due to autometasomatism process. Mineralogically, the lamprophyre is classified into monchiquite alkaline lamprophyre (see also in Figure 1).

Geochemical Features

The results of major and trace element analyses of five komatiitic lamprophyric samples are shown in Table 2. The lamprophyric rocks have relatively high LOI values (~4.55 wt %) which indicate the presence of higher primary volatiles (e.g. CO_2, Cl, F, etc.), but plot on ternary MIA(o) diagram (Figure 5) displaying s unweathered rock. The lamprophyric rock have characteristics of low SiO_2 contents 46.43 - 47.80 %), high in MgO (10.02 - 12.67 %), relatively high in alkaline (Na_2O: 2.20 - 2.59 %; K_2O: 1.58 - 2.45 %; Total alkali: 4.00 - 4.89 %), CaO (9.29 - 10.71 %), and relatively low of alumina (Al_2O_3 : 10.98 - 11.70 %), TiO_2 (0.84 - 1.00 %), FeOt (7.75 - 7.88 %). By plotting the values of MgO, K_2O, and Al_2O_3 on the Bergman (1987) triangular diagram (Figure 6), the rocks studied fall on lamprophyres. The ratio of MgO/Al_2O_3: 0.86 - 1.00 ("> 0.7906") ensures the geochemical affinities with typical komatiitic composition indicating the unfractionation magma (Jensen, 1976; Figure 7). The komatiitic lamprophyre has a high Mg#= 69 - 74 which proves that the protolith was originated from mantle melt (after Schilling *et al.*, 1983; Figure 8). The relatively low content of $TiO_2 < (-1.1610 + 0.1935 \times Al_2O_3$; in wt. %) indicates the typical of geotectonic is more towards Arc-related (Muller and Groves, 1993 and 2000; Figure 9).

Interpretation of Results

The analytical results of various diagrams have been plotted on a diagram to classify high-Mg komatiitic lamprophyric rock and to explain

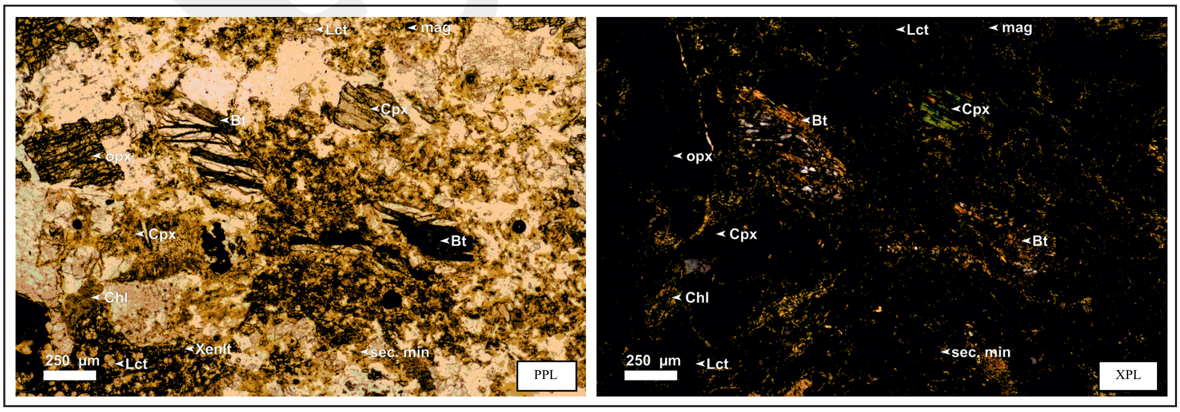

Figure 4. Photomicrographs of representative sample which interpreted as alkaline monchiquite lamprophyre. PPL: plane polarized; XPL: x-polarized; Chl: chlorite; Bt: biotite; Lct: leucite; Cpx: clinopyroxene; mag: magnetite; opx: orthopyroxene; sec.min: secondary minerals.

Table 2. Analysis Results of Major Oxides (wt.%), Trace and REE (ppm) of Komatiitic Lamprophyric Samples

Code#	#1	#2	#3	#8	#9	#15	#16	#17	#18
Location			**Western Sulawesi**			**Yunnan, China**	**Rock, 1991**	**Western Jawa**	
Rock names	**Komatiitic lamprophyre**	**Komatiitic lamprophyre**	**Komatiitic lamprophyre**	**Komatiitic lamprophyre**	**Komatiitic lamprophyre**	**Donggualin lamprophyre**	**Alkaline lamprophyres**	**Galunggung Basalt**	**Galunggung Basalt**
Sample_code	**#A01_2012**	**#A02_2012**	**#A03_2012**	**#B01_2016**	**#B02_2016**	**n5**	**n854**	**Gal132a**	**Gal132b**
SiO_2 (%)	47.23	47.70	46.43	47.40	47.80	46.67	42.50	49.14	49.06
TiO_2	1.00	0.94	0.84	0.97	0.92	0.54	2.90	0.83	0.84
Al_2O_3	11.70	11.07	11.66	11.64	10.98	12.84	13.70	15.93	15.93
Fe_2O_3(t)	8.61	8.70	8.61	8.75	8.76	6.42	12.00	10.32	10.18
FeO									
MnO	0.14	0.15	0.15	0.14	0.15	0.13	0.20	0.17	0.17
MgO	10.02	10.84	12.67	10.09	10.93	8.22	7.10	10.33	10.14
CaO	10.11	10.71	9.29	10.18	10.78	7.75	10.30	11.19	11.15
Na_2O	2.59	2.22	2.42	2.55	2.20	1.48	3.00	2.23	2.19
K_2O	2.30	2.45	1.58	2.30	2.42	4.83	2.00	0.36	0.36
H_2O+						2.24	3.10		
H_2O-						0.19			
CO_2						8.23	2.00		
LOI				5.00	4.10			-0.51	-0.49
P_2O_5	0.83	0.82	0.81	0.82	0.81	0.56	0.74	0.10	0.10
Total	94.53	95.60	94.45	99.84	99.84	100.09	99.54	100.09	99.63
TA=Na_2O+K_2O	**4.89**	**4.67**	**4.00**	**4.85**	**4.62**	**6.31**	**5.00**	**2.59**	**2.55**
K_2O/Na_2O	**0.89**	**1.10**	**0.65**	**0.90**	**1.10**	**3.27**	**0.67**	**0.16**	**0.16**
S (%)				0.19	0.17	0.20			
Cr_2O_3 (%)				0.04	0.05				
Mg#	**69.74**	**71.16**	**74.45**	**69.55**	**71.19**	**71.70**	**53.96**	**66.47**	**66.36**
MgO/Al_2O_3	**0.86**	**0.98**	**1.09**	**0.87**	**1.00**	**0.64**	**0.52**	**0.65**	**0.64**
F							1,800.00		
Cl							330.00		
Cr	279.00	326.00	411.00	284.00	268.00	431.75	97.00	541.00	521.50
Cu				76.00	75.00	29.88	50.00		
Ni	102.00	121.00	256.00	105.00	119.00	195.33	65.00	163.10	157.80
Sc				41.00	43.00	24.00	21.00	39.70	39.00
Ti				5,800.00	5,390.00				
V				212.00	211.00	121.75	285.00	269.30	265.60
Zn				60.00	55.00	56.73	98.00		
Ag				0.20	0.20				
As				5.00	5.00		2.00		
Ba				2,270.00	1,680.00	1,916.00	930.00	85.20	88.10
Be				3.60	3.90		1.00		
Bi				0.46	0.30				
Cd				0.28	0.37				
Co	37.00	37.00	42.00	37.00	37.00	27.40	38.00		
Cs				10.20	8.20		2.00	0.58	0.63
Ga				14.80	14.80		19.00	15.30	16.10
Ge				1.60	1.50				
Hf				5.20	5.60	4.44	6.90	1.23	1.23
In				0.06	0.05				
Li				6.20	8.00		24.00		
Mo				1.20	0.60		8.50		
Nb				12.40	11.90	8.09	101.00	1.80	2.20
Pb				43.00	50.00		7.00	3.80	3.90
Rb				137.00	114.00	199.50	50.00	7.50	7.50
Re				<0.05	<0.05				
Sb				0.40	0.50				
Se				<1	<1				
Sn				3.70	3.60				

Table 2. Continued....

Code#	#1	#2	#3	#8	#9	#15	#16	#17	#18
Location	Western Sulawesi					Yunnan, China	Rock, 1991	Western Jawa	
Rock names	Komatiitic lamprophyre	Komatiitic lamprophyre	Komatiitic lamprophyre	Komatiitic lamprophyre	Komatiitic lamprophyre	Donggualin lamprophyre	Alkaline lamprophyres	Galunggung Basalt	Galunggung Basalt
Sample_code	#A01_2012	#A02_2012	#A03_2012	#B01_2016	#B02_2016	n5	n854	Gal132a	Gal132b
Sr				499.00	552.00	844.00	990.00	208.20	207.40
Ta				0.77	0.84	0.59	5.00	0.13	0.13
Te				<0.1	<0.1				
Th				25.60	26.50	11.59	9.00	0.82	0.82
Tl				1.57	1.45				
U				5.49	5.04	4.21	2.20	0.19	0.20
W				2.50	2.60		2.50		
Zr				162.00	175.00	121.10	313.00	46.00	46.50
La				38.50	42.90	33.73	66.00	4.03	4.12
Ce				84.80	92.90	68.59	125.00	9.60	9.65
Pr				10.20	10.90	8.76	14.00	1.49	1.49
Nd				40.40	42.80	34.07	54.00	7.15	7.16
Sm				7.50	8.00	6.64	10.80	2.05	2.05
Eu				1.70	1.70	1.71	3.10	0.78	0.80
Gd				6.80	7.30	5.41	8.20	2.71	2.75
Tb				0.71	0.80	0.74	1.20	0.45	0.45
Dy				3.90	4.00	4.04	5.40	2.69	2.72
Ho				0.70	0.70	0.71	0.90	0.55	0.54
Er				1.80	1.90	1.86	2.70	1.61	1.62
Tm				0.20	0.20	0.27	0.38	0.25	0.25
Yb				1.70	1.70	1.63	1.80	1.58	1.57
Lu				0.28	0.28	0.24	0.29	0.26	0.26
Y				19.10	20.20	18.91	31.00	16.90	16.90
TRE				**218.29**	**236.28**	**187.30**	**324.77**	**52.10**	**52.33**
TREO				**244.05**	**264.15**	**209.54**	**363.34**	**58.95**	**59.21**
TRExOy				**262.18**	**283.82**	**224.93**	**390.32**	**62.99**	**63.26**
TRE_2O_3				**256.93**	**278.08**	**220.66**	**382.62**	**62.38**	**62.64**
dEu				**0.73**	**0.68**	**0.87**	**1.01**	**1.01**	**1.03**
dCe				**1.04**	**1.04**	**0.97**	**1.00**	**0.95**	**0.94**

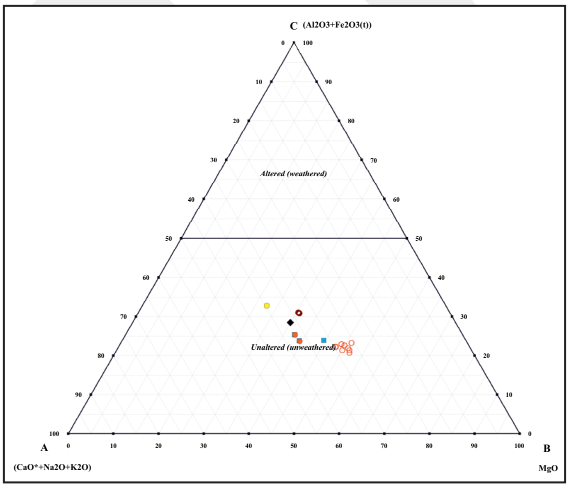

Figure 5. Ternary Mafic Index of Alteration diagram MIA(o); after Nesbitt and Wilson, 1992; modified by Babechuk *et al.*, 2014. ($CaO^*+Na_2O+K_2O$), MgO and ($Al_2O_3+Fe_2O_3$(t)), (in molar).

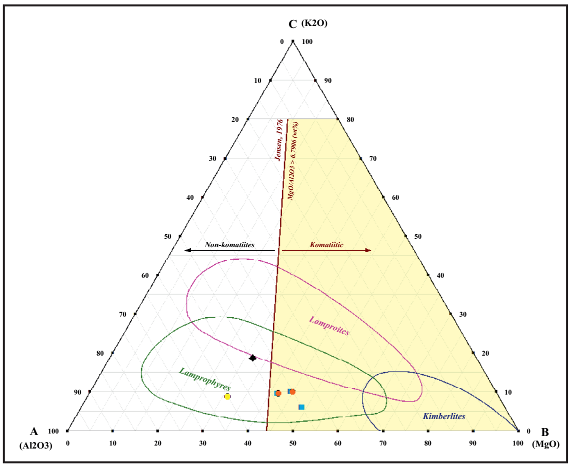

Figure 6. Ternary discrimination for Lamprophyres–Lamproites–Kimberlites (Al_2O_3–MgO–K_2O, in wt%; after Bergman, 1987). The field of the discrimination of komatiitic and non-komatiites (MgO/Al_2O_3 = 0.7906, in wt%) is mathematically converted from Jensen (1976).

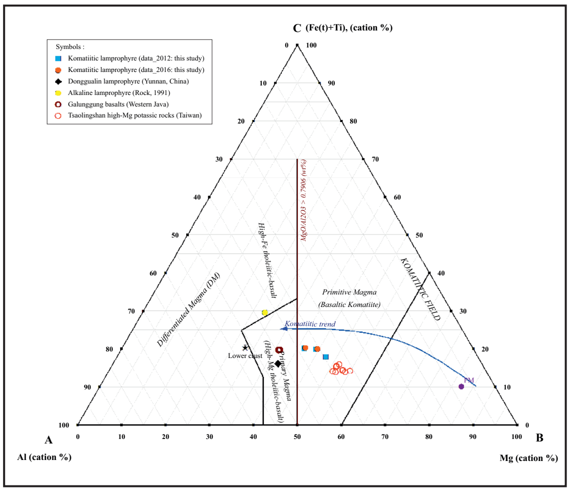

Figure 7. Ternary cation plot for classifying Komatiitic [Primitive Mantle (PM) and Primitive Magma], Primary Magma, and Differentiated Magma (DM) (after Jensen, 1976).

their tectonic setting and protoliths that lead to their formation.

The plot of K_2O/Na_2O ratio with values of 0.65 to 1.10 in Trapezoid Magmatic Alkalinity diagram falls within shoshonitic series field (Godang *et al*., 2016; Figure 10). The interpretation is similar to the plot result in diagram of Peccerillo and Taylor (1976) Figure 11). The approach with multigeotectonic basalt diagrams developed from Hollocher *et al*., 2012a (after Sun *et al*., 2006, modified by Godang *et al*. (2016); Pearce, 2008) (Figures 12 - 14) shows that the whole diagram presents the tectonic setting of komatiitic shoshonitic lamprophyre is in the form of 'alkaline continental-arc' or 'continental within-plate'. The overlay between the diagram of Figure 9 and Figures 12 - 14 could be proposed the geotectonic was formed in 'alkaline continental-arc'. As a comparison, the geochemical data for shoshonitic alkaline lamprophyre has been plotted from Lamprophyres textbook (Rock, 1991) into the same Figures 12 - 14 and Figure 9, which shows the rock fall within a mantle plume field and within-plate. These reveal the alkaline lamprophyres could be generated from different tectonic setting.

Melting Conditions and the Interpretation of the Protoliths

Geochemical compositions of parental magmas have widely been used for estimating mantle

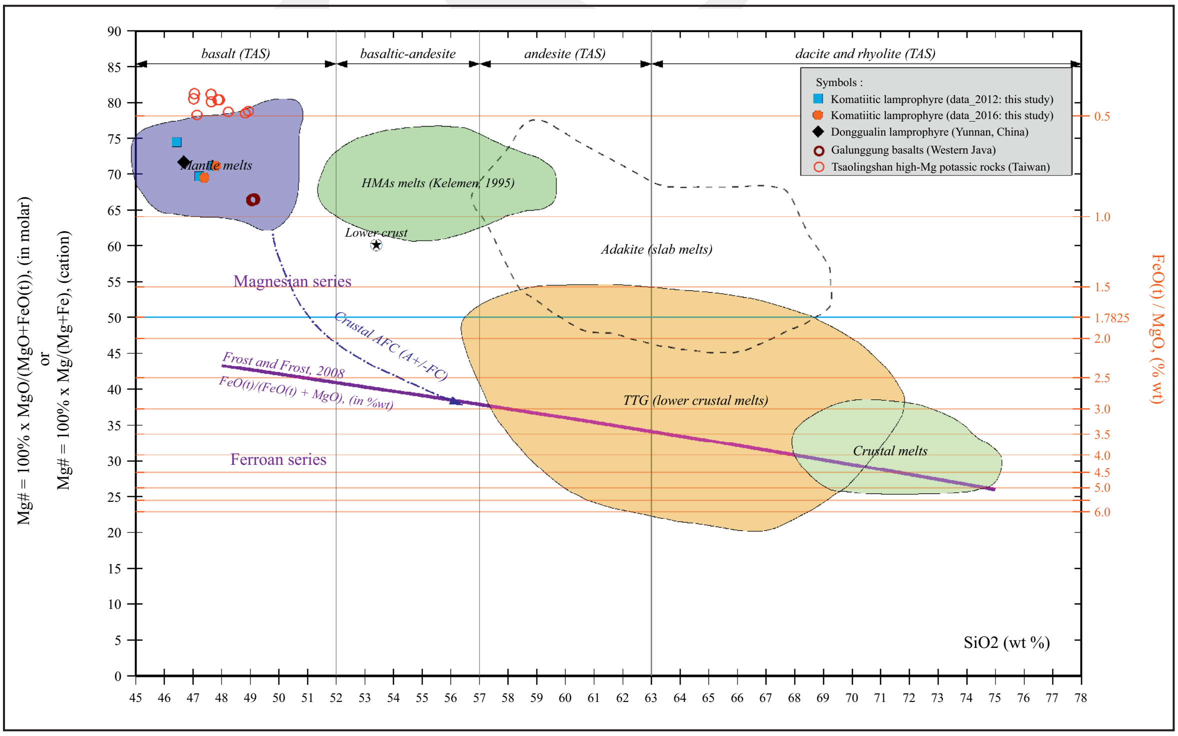

Figure 8. Index of differentiation diagram (Mg#; after Schilling *et al*., 1983), mantle-melts is taken from Kinzler (1997), crust-melts (Dokuz, 2011), high-Mg andesites melts (HMAs; Kelemen, 1995), TTG (lower-crustal melts) and adakite (slab melts) are taken from Condie (2005); the discrimination of magnesian series *vs* ferroan series (Frost and Frost, 2008).

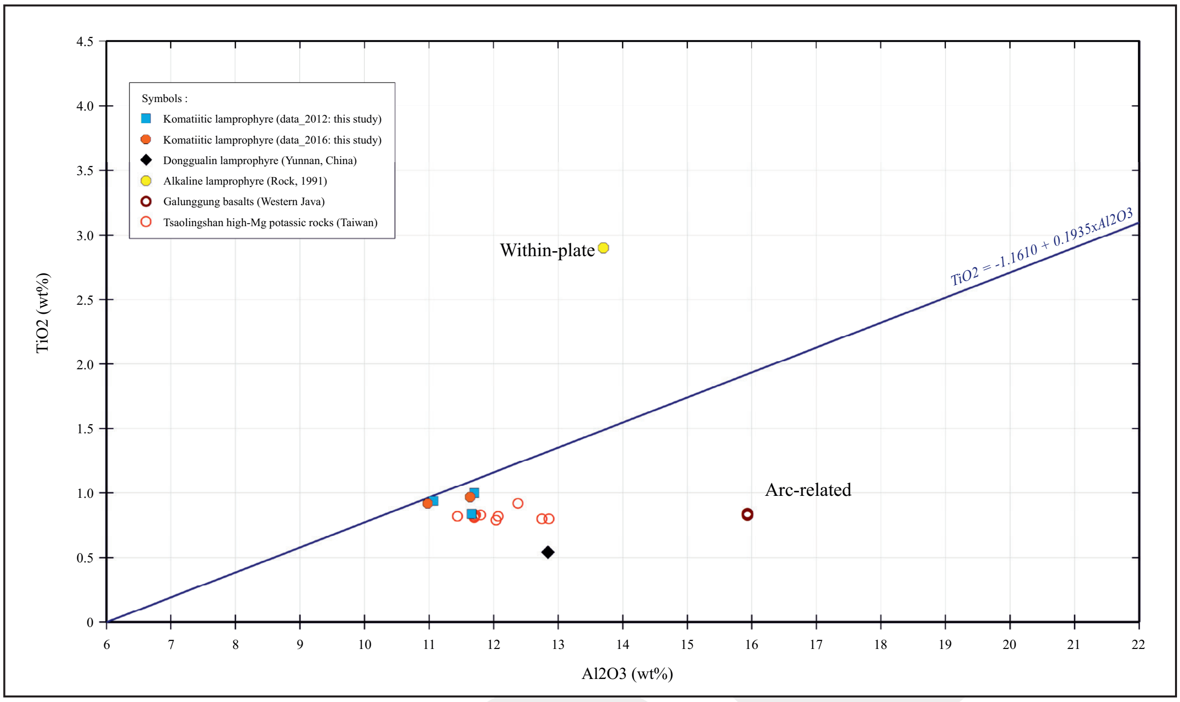

Figure 9. Geotectonic diagram for discrimination Within-plate *vs* Arc-related (Muller and Groves, 1993 and 2000). The Alkaline lamprophyre (Rock, 1991) formed in within-plate tectonic setting (Anorogenic); whereas Komatiitic lamprophyre (this study), Donggualin lamprophyre (China), Tsaolingshan high-Mg potassic rocks (Taiwan), and Galunggung basalts (western Jawa) were formed in the tectonic of Arc-related (Orogenic).

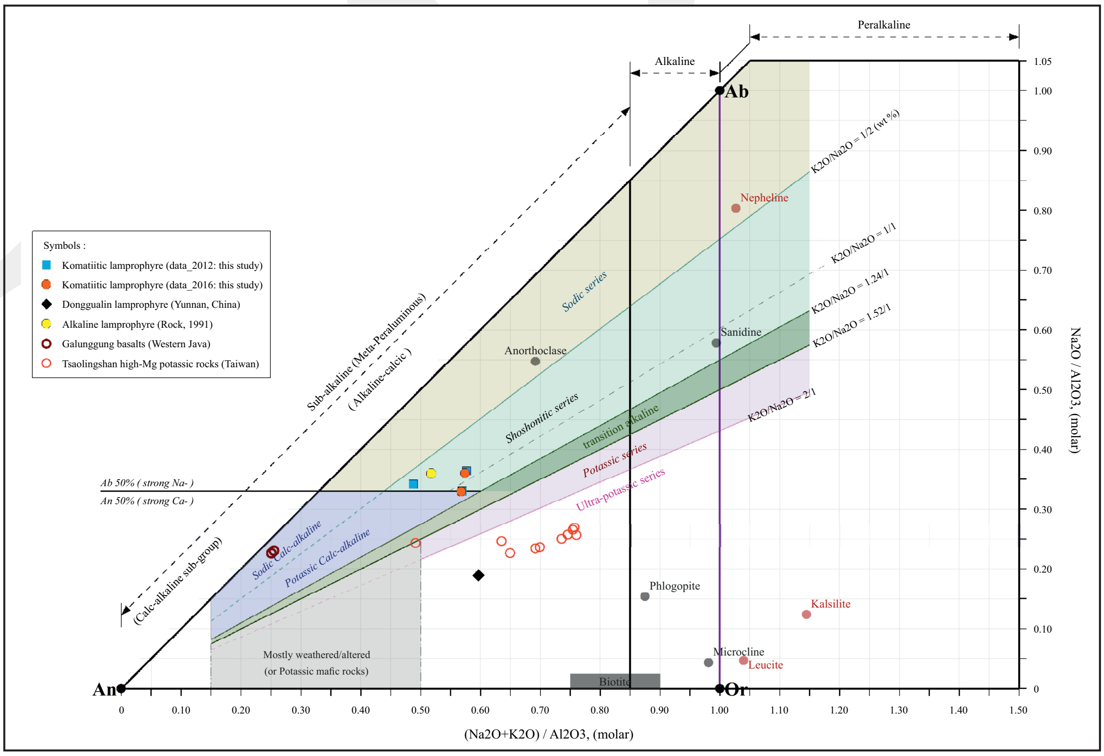

Figure 10. Trapezoid Magmatic Alkalinity Classification (Godang *et al*., 2016). Plots show western Sulawesi komatiitic lamprophyre (this study) and alkaline lamprophyre (Rock, 1991; p.78) fall in shoshonitic series, China Yunnan Donggualin lamprophyre shows ultra-potassic series, Taiwan Tsaolingshan high-Mg rocks shows potassic/ultra-potassic series and Galunggung basalt (western Jawa) fall in field calc-alkaline sub-group (it may be in form of sodic calc-alkaline or tholeiitic).

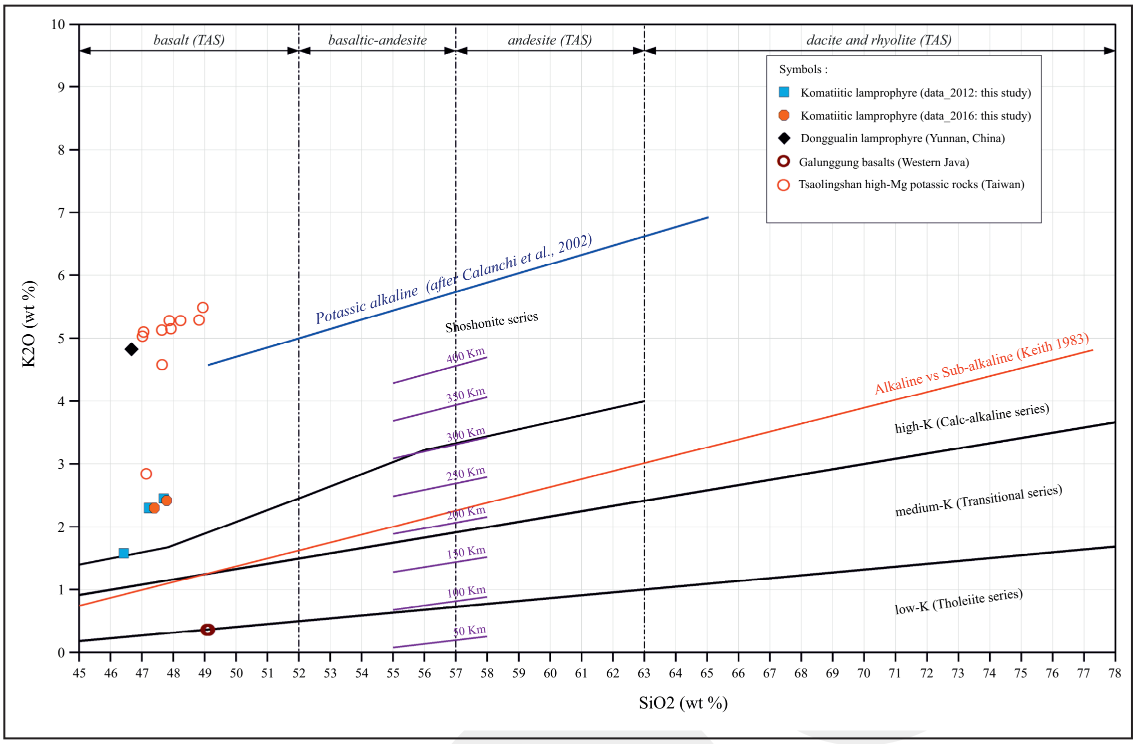

Figure 11. Volcanic rocks classification for orogenic zone (K_2O *vs* SiO_2, wt%; after Peccerillo and Taylor, 1976). The depth to Benioff Zone {after Hatherton and Dickinson, 1969; modified by Fadlin and Godang, 2015 (in Godang *et al*., 2016)}.

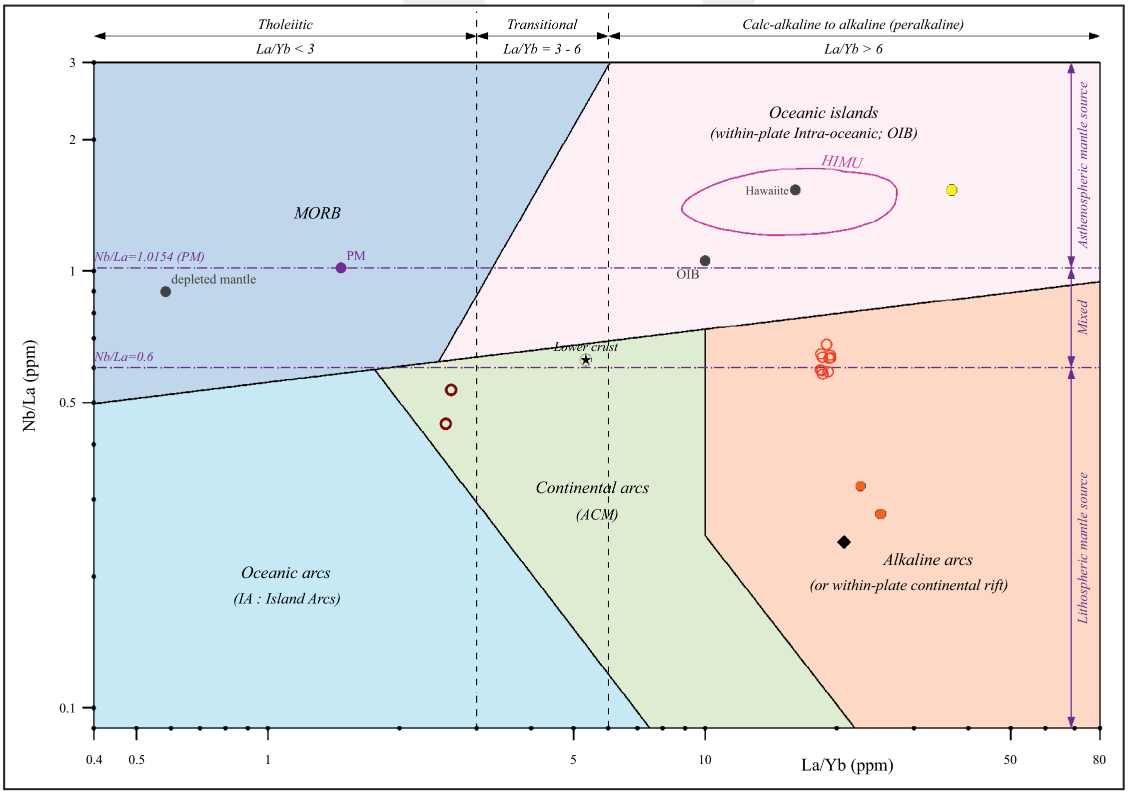

Figure 12. Tectonic discrimination diagram for Basalts (after Hollocher *et al*., 2012a). Magmatic Affinity: ratio La/Yb for Tholeiitic--Transitional--Calc-alkaline to Alkaline (MacLean and Barrett, 1999); ratio Nb/La for Lithospheric and Asthenospheric mantle is adopted from after Abdel-rahman (2002). Symbol in Figure 7.

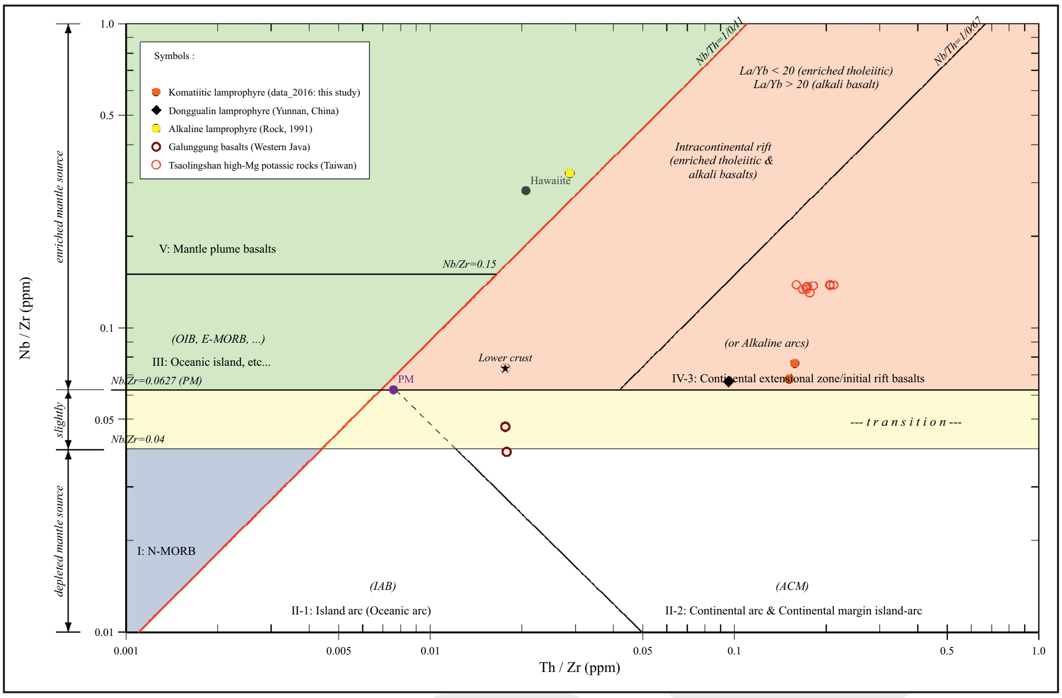

Figure 13. Tectonic discrimination diagram for basalts (after Sun *et al.*, 2006; modified from Godang *et al.*, 2016). After overlaying with Figure 9, it could be proposed the geotectonic of Western Sulawesi komatiitic monchiquite lamprophyre, China Yunnan Donggualin lamprophyre and Taiwan Tsaolingshan high-Mg potassic rocks were formed in 'Supra-subduction alkaline continental-arc'; Galunggung basalt was formed in ACM, and Alkaline lamprophyre (Rock, 1991) was formed in mantle plume.

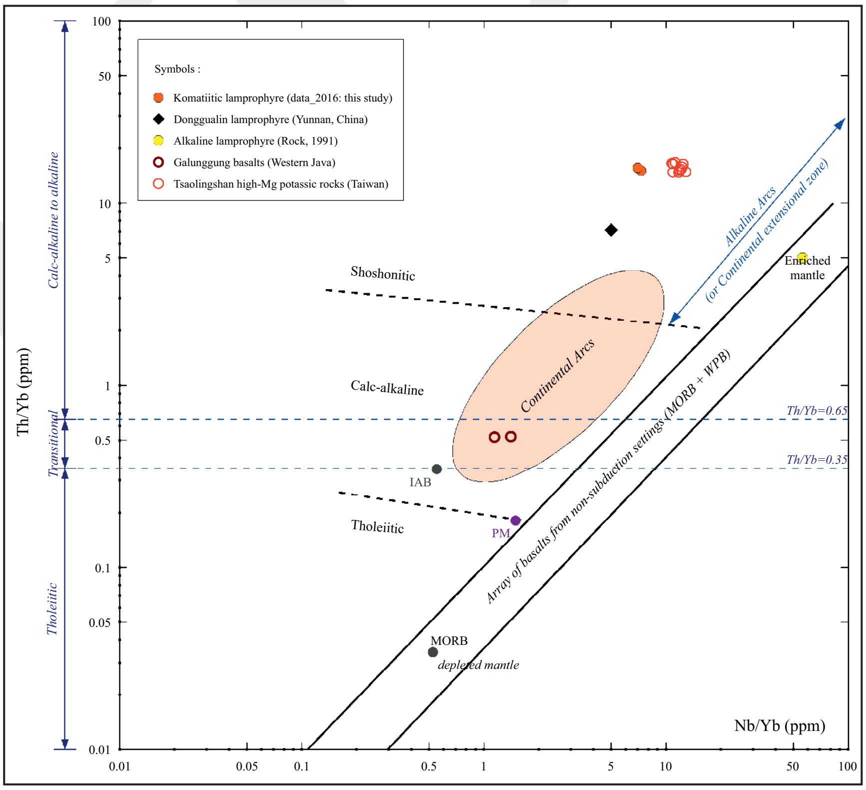

Figure 14. Discriminants for Mantle melting array *vs.* Arc basalts (after Pearce, 2008). Magmatic affinity: the ratio Th/Yb (MacLean and Barrett, 1993).

melt conditions. To minimize the chemical effects of crustal contamination, the calculation was started with the least-evolved of sample#3 which has the highest MgO (12.67 %), Ni (256 ppm), Cr (411 ppm), and the lowest SiO2 (46.43 %). MgO concentration on primary basaltic melts is directly related to melt temperatures (e.g. Albarède, 1992; Herzberg *et al.*, 2007). The melt temperature of the West Sulawesi komatiitic lamprophyres was calculated at 1,397°C using the equation proposed by Albarède, 1992 {T(°C)= 2000 x MgO/(MgO + SiO_2)(wt %) + 969}, consistent with the estimation 1,393°C by using the equation {T(°C)= 1463 + 12.74 x MgO – 2924 /MgO (wt%)}(Herzberg *et al.*, 2007; Figure 15). The plot on diagram by using correlation between T(°C) and MgO (wt %) shows the MELTS temperature was 1,362°C (Asimow *et al.*, 2001; Figure 15). The lamprophyric samples have a relatively low concentration of Al_2O_3 (10.98 - 11.70 wt %), and have the ratio of CaO/Al_2O_3 around 0.80 - 0.98 which is consistent with the segregation of primary magmas at 3.5 - 3.8 GPa, and it is estimated to occur at a depth about 120 km (Figure 16; Herzberg, 1995 and Ghiorso and Sack, 1995).

The correlation between Ni and MgO concentrations is displayed in Figure 17 (after Wang *et al.*, 2007). The diagram shows that the komatiitic lamprophyric magma is dominantly controlled by olivine fractional crystallization. The plot in Figure 18 (diagram after Aldanmaz *et al.*, 2000 and 2006) suggests the komatiitic lamprophyre is derived from the enriched mantle source (Nb/Zr > 0.0627), and the magma was generated from partial melting of DMM (depleted MORB mantle) which composed of pyroxene-peridotite (garnet-lherzolite). This finding is consistent with the previous paper from Godang *et al.*, 2016. As a comparison, the plot data for primary magma of Galunggung

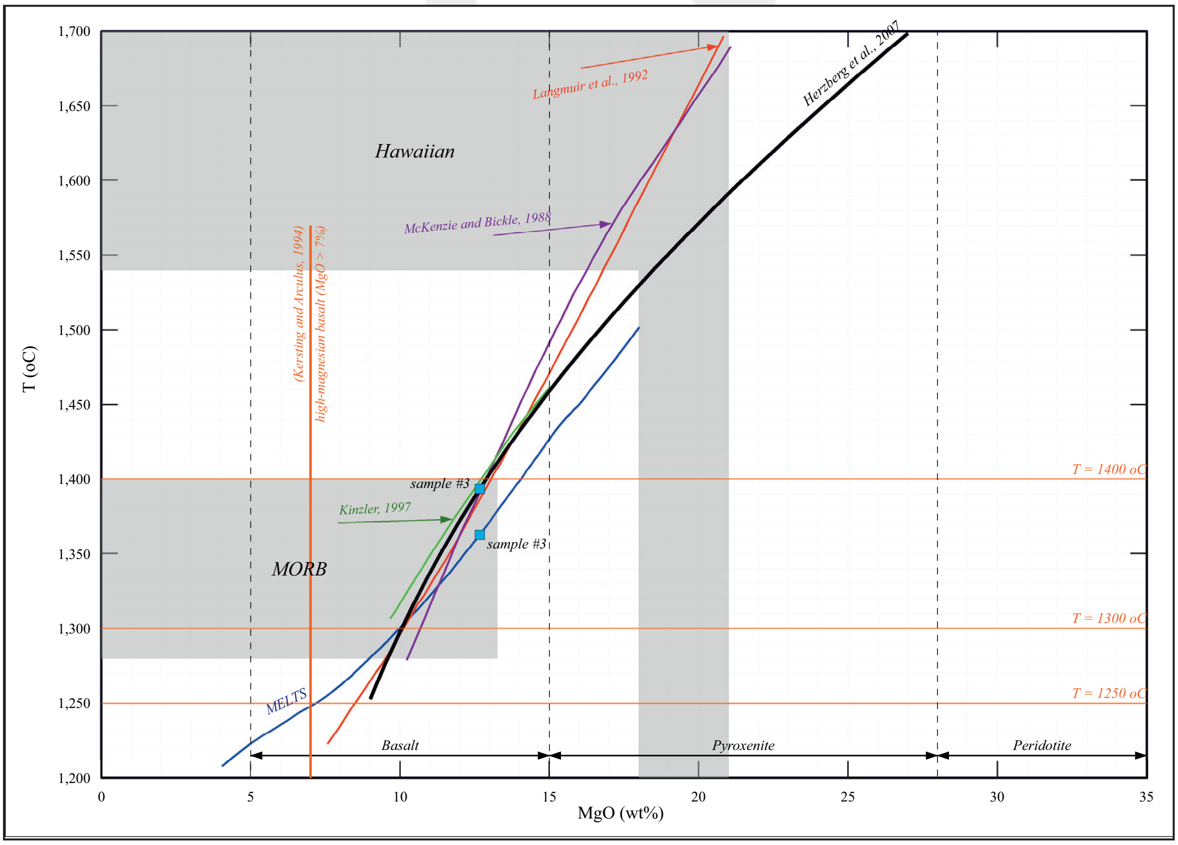

Figure 15. Mantle potential temperatures (Tp, °C) as a function of the MgO concentrations of primary magmas (after Herzberg *et al.*, 2007). MELTS blue solid line (Asimow *et al.*, 2001). Plots show the melting temperature of komatiitic lamprohyre (sample #3, MgO = 12.67%) occurs at >1350°C.

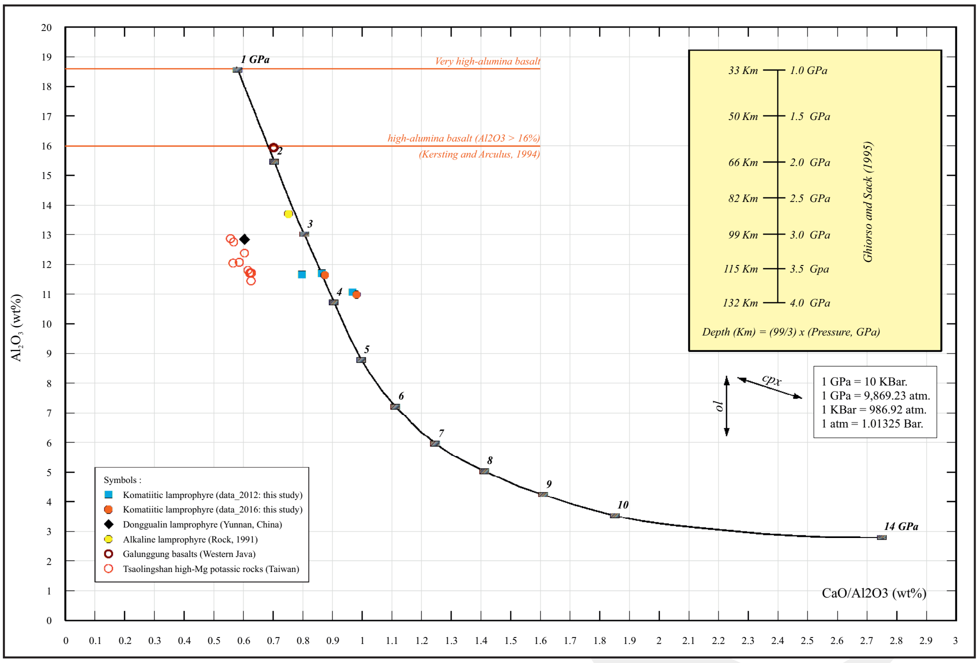

Figure 16. Pressure of Magmatic Segregation Diagram (Herzberg, 1995). Al_2O_3 *vs*. CaO/Al_2O_3 in wt%. Plots show the melting pressure of Western Sulawesi komatiitic lamprophyre at 3.5–3.8 GPa with an estimated of depth = (3.5+3.8)/2 x (99/3) = 120.45 Km (~120 Km).

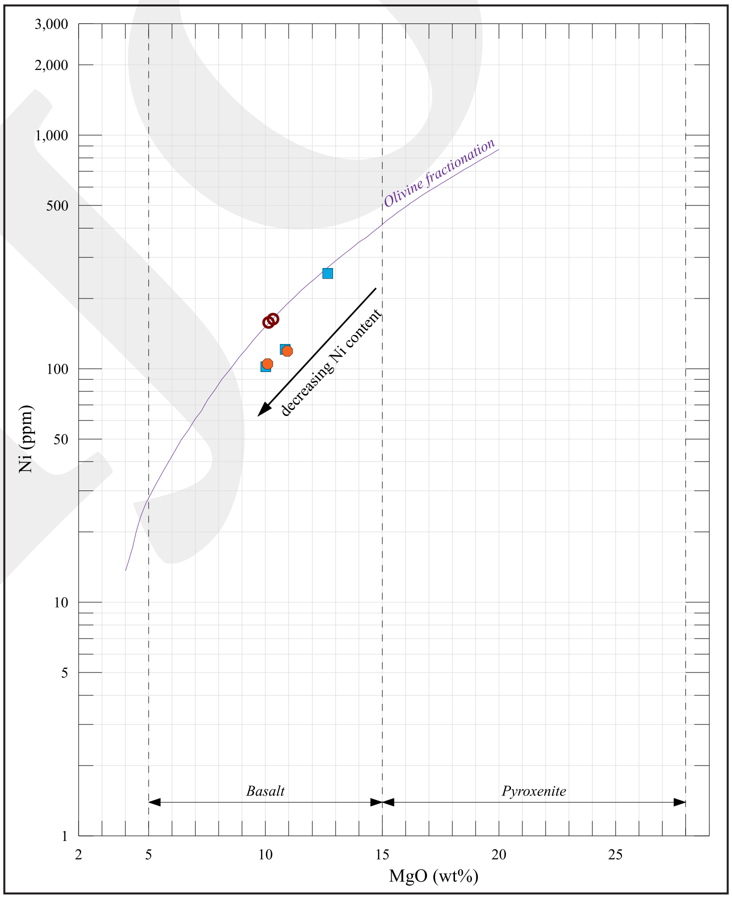

Figure 17. Plots of Ni *vs*. MgO (after Wang *et al.*, 2007) show Western Sulawesi komatiitic lamprohyre and Galunggung basalts form a tight linear trend dominantly controlled by olivine fractional crystallization. Symbols in Figure 7.

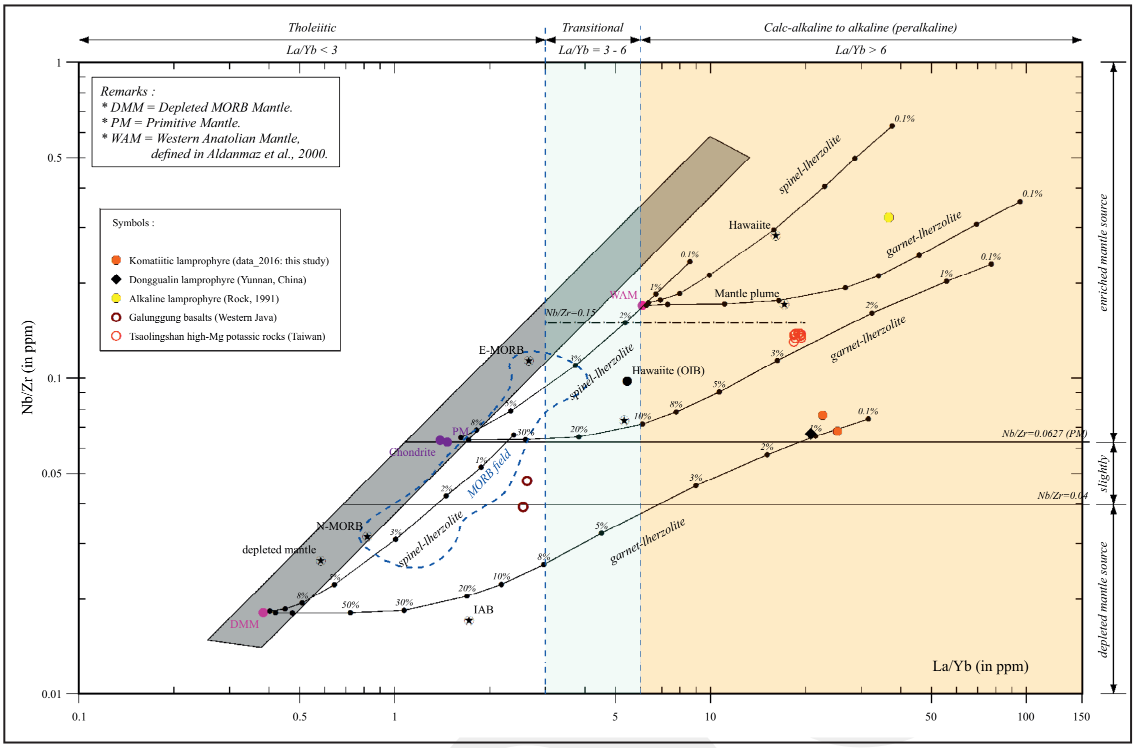

Figure 18. Partial melting curves of mantle source (after Aldanmaz *et al*., 2000 and 2006). Magmatic affinity: the ratio of La/Yb (MacLean and Barrett, 1993), the ratio of Nb/Zr for discriminating depleted--slightly--enriched mantle is adopted from Le Roex *et al*. (1983) and Sun *et al*. 2006.

basalts, West Java (SiO_2: 49.06 - 49.14 %; high MgO: 10.14 - 10.33 %) show the magma was generated from the same of DMM, but it has a slightly enriched mantle source (0.0627 > Nb/Zr > 0.04), and composed of the mixing between spinel and garnet-lherzolite.

Discussion

The results show the West Sulawesi monchiquite lamprophyre is represented by shoshonitic magma series with komatiitic composition, which generated from the lithospheric mantle melts formed in a suprasubduction alkaline continental-arc tectonic setting (see also in Table 3). The source of magmatism proposed comes from the suprasubduction activities from the east. Furthermore, the partial melting of monchiquite lamprophyre estimating was formed in high pressure of 3.5 - 3.8 GPa with melting temperature of >1350°C.

Referring to the spidergram pattern in Figure 19, West Sulawesi komatiitic lamprophyre has a similar trend with China Yunnan Donggualin lamprophyre (Huang et al., 2002), but has a little bit higher of Th content, and the difference in the ratio of MgO/Al_2O_3. The komatiitic lamprophyre (this study) has a ratio of MgO/Al_2O_3 > 0.7901, whereas the China Yunnan Donggualin lamprophyre has a ratio of MgO/Al_2O_3= 0.64 which indicates nonkomatiitic lamprophyre (Figure 7). The komatiitic lamprophyre has also a different pattern with the textbook of alkaline lamprophyre (Rock, 1991). Furthermore, the alkaline lamprophyre (Rock, 1991) has a similar trend with Hawaiite mantle plume (sodic series; Chakraborty, 2007). The similarities or inequality patterns of lamprophyres may be due to the differences in genesis and/or protoliths. West Sulawesi komatiitic lamprophyre in spidergram pattern (Figure 20) shows the negative Eu anomaly (dEu = 0.68 - 0.73), and it is characterized by distinctly negative spikes in Nb-Ta, Ti, and has enriched

Table 3. Various Geotectonic Settings from Primary and Differentiated Magma Sources

	Rock sources	Primary magma/ koma titic	Mantle melts	Magmatic alkalinity	Geotectonic setting	Protoliths
	Figures	**Figure 7**	**Figures 7, 8, 12**	**Figures 10 - 11**	**Figures 9, 12 - 14**	**Figure 18**
A	Galunggung basalts, Western Java (Dempsey, 2013)	Primary magma (Non-komatiitic)	Lithospheric mantle melts	Tholeiitic	ACM, magma comes from the subcontinental lithospheric mantle melts (mantle wedge melts)	DMM (mix spinel and garnet-lherzolite)
B	Donggualin lamprophyre, Yunnan-China (Huang *et al.*, 2002	Primary magma (Non-komatiitic)	Lithospheric mantle melts	Ultra-potassic	Supra-subduction alkaline continental-arc	DMM (garnet-lherzolite)
C	Alkaline lamprophyre (Rock, 1991)	Differentiated magma	Fractionated magma from asthenospheric mantle sources	Shoshonitic	Mantle plume (within-plate)	WAM (mix spinel and garnet-lherzolite)
D	Western Sulawesi monchiquite lamprophyre (this study)	Komatiitic ($MgO/Al_2O_3 > 0.7906$)	Lithospheric mantle melts	Shoshonitic	Supra-subduction alkaline continental-arc	DMM (garnet-lherzolite)
E	Tsaolingshan high-Mg potassic rock, Taiwan (Chung *et al.*, 2001)	Komatiitic ($MgO/Al_2O_3 > 0.7906$)	Mix lithospheric and asthenospheric mantle melts	Potassic/ Ultra-potassic	Supra-subduction alkaline continental-arc	PM (garnet-lherzolite)

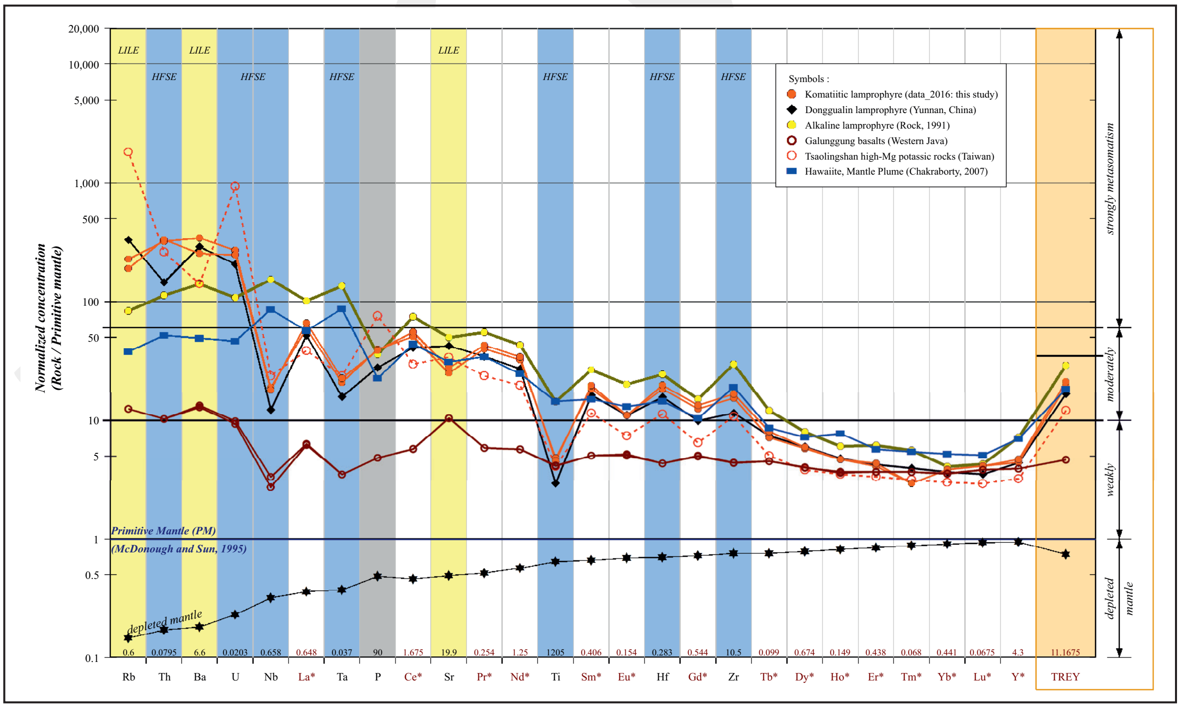

Figure 19. Incompatible to compatible multi-trace elements diagram Normalized to Primitive Mantle (the incompatibility sequence is referred from Zhang, 2014). The description of weakly-moderately-strongly mantle metasomatism is only used for the determination of metasomatism level of mafic rocks (modified from Godang *et al*., 2016). Primitive Mantle (PM) values are taken from McDonough and Sun (1995) and Depleted Mantle (DM) from Salters and Stracke (2004), showing plots of Western Sulawesi komatiitic lamprophyre have a similar pattern with China Yunnan Donggualin lamprophyre. The alkaline lamprophyre (Rock, 1991) have a similar trend with Hawaiite mantle plume (sodic series). Taiwan Tsaolingshan high-Mg potassic rock has a different pattern with Sulawesi komatiitic lamprophyre (this study), Yunnan Donggualin lamprophyre, Alkaline lamprohyre (Rock, 1991), and Hawaii mantle plume. The Galunggung basalt (tholeiitic primary magma) has a lower value of trace elements and REE (in TREY).

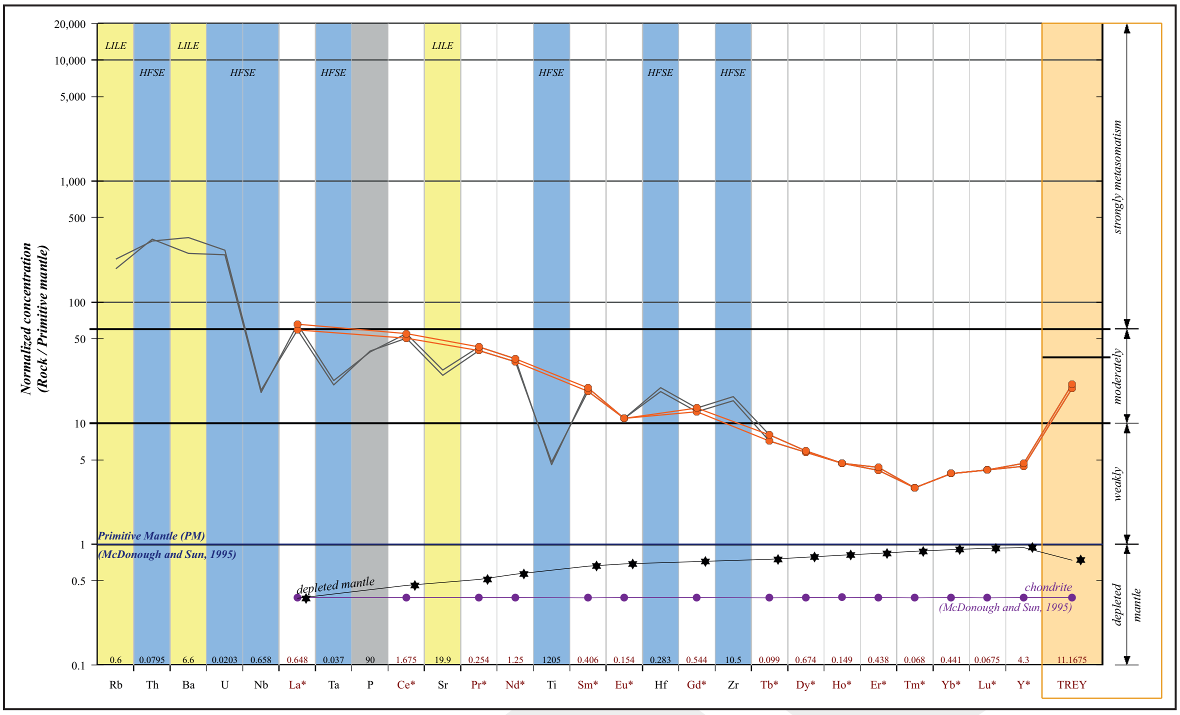

Figure 20. The overlay of Normalized to Primitive Mantle diagram between Rare Earth Elements (REEs) and trace elements. The grey solid line is copied from Figure 19, orange solid line is REEs. The chondrite values are taken from McDonough and Sun (1995) and Depleted Mantle (DM) from Salters and Stracke (2004). The diagram shows Western Sulawesi komatiitic lamprophyre has a negative Eu anomaly (dEu = 0.68 - 0.73) followed by the enrichment of light-REE (La, Ce, Pr, Nd, Sm) and TREY. Furthermore, it is characterized by distinctly negative spikes in Nb-Ta, Ti, and has enriched in other High Field Strength Elements (HFSE), i.e. Th-U, Zr-Hf.

in Th-U, Zr-Hf, light-REE (La, Ce, Pr, Nd, Sm), and TREY.

Conclusion

The integrated petrographic, mineralogical, and geochemical studies of komatiitic shoshonitic lamprophyre have obtained the following conclusions:

- West Sulawesi lamprophyre is classified into monchiquite lamprophyre with needle-like texture, indicating the unfractionated komatiitic primitive magma with shoshonitic alkalinity magma series.
- Geotectonic setting of the lamprophyric rock was formed in suprasubduction alkaline continental-arc, which the magmatism came from the suprasubduction activities from the east.
- The protoliths of komatiitic lamprophyric magma was generated from partial melting of depleted MORB mantle (DMM), comprising pyroxene-peridotite (garnet-lherzolite).
- The partial melting conditions are suggested to occur at high pressure (3.5 - 3.8 GPa) and depth of about 120 km with the melting temperature of >1350°C, and the magma is dominantly controlled by olivine fractional crystallization.

Acknowledgments

The authors express their gratitude to P.T. Monazite Fushi for giving a permit to conduct the fieldwork for this study. The authors are thankful to Dr. I Wayan Warmada (Department of Geological Engineering, Gadjah Mada University) for the petrographic analysis.

References

Abdel-rahman, A.M., 2002. Mesozoic volcanism in the Middle East: geochemical, isotopic, and petrogenic evolution of extension related alkali basalts from central Lebanon. *Geological Magazine,* 139 (6), p.621-640. DOI:10.1017/s0016756802006829

Albarède, F., 1992. How deep do common basaltic magmas form and differentiate? *Journal of Geophysical Research*, 97, p.10, 997-11,009. DOI:10.1029/91jb02927

Aldanmaz, E., Pearce, J.A., Thirlwall, M.F., and Mitchell, J.G., 2000. Petrogenetic evolution of Late Cenozoic, post-collision volcanism in western Anatolia, Turkey. *Journal of Volcanology and Geothermal Research,* 102, p.67-95. DOI: 10.1016/S0377-0273(00)00182-7.

Aldanmaz, E., Koprubasi, N., Gurer, O.F., Kaymakci, N., and Gourgaud, A., 2006. Geochemical constraints on the Cenozoic, OIB-type alkaline volcanic rocks of NW Turkey: Implications for mantle sources and melting processes. *Lithos,* 86, p.50-76. DOI: 10.1016/j.lithos.2005.04.003.

Arndt, N. T. and Nisbet, E. G., 1982. What is a komatiite? *In*: Arndt, N.T. and Nisbet, E.G. (eds), *Komatiites*, London, George Allen and Unwin, p.19-28. DOI:10.1180/minmag.1983.047.345.24

Asimow, P.D., Hirschmann, M.M., and Stolper, E.M., 2001. Calculation of peridotite partial melting from thermodynamic models of minerals and melts, IV. Adiabatic decompression and the composition and mean properties of mid-ocean ridge basalts. *Journal of Petrology*, 42, p.963-998. DOI:10.1093/petrology/42.5.963

Babechuk, M.G., Widdowsonc, M., and Kamber, B.S., 2014. Quantifying chemical weathering intensity and trace element release from two contrasting basalt profiles, Deccan Traps, India. *Chemical Geology,* 363, p.56-75. DOI:10.1016/j.chemgeo.2013.10.027

Bergman, S.C., 1987. Lamproites and other potassic igneous rocks: A review of their occurrence, mineralogy and geochemistry. *In*: Fitton, J.G. and Upton, B.G.J. (eds.), *Alkaline Igneous Rocks*, Geological Society Special Publication, 30, p.103-190. DOI:10.1144/gsl.sp.1987.030.01.08

Carlson, R.W. and Nowell, G.M., 2001. Olivine-poor sources for mantle-derived magmas: Os and Hf isotopic evidence from potassic magmas of the Colorado Plateau. G3 (*An Electronic Journal of the Earth Sciences*), 2. DOI:10.1029/2000gc000128

Chakraborty, S., 2007. *The Geochemical Evolution of Alkaline Magmas from the Crary Mountains, Marie Byrd Land, Antarctica. Master of Science Thesis*. Bowling Green State University.

Chung, S.L., Wang, K.L., Crawford, A.J., Kamenetsky, V.S., Chen, C.H., Lan, C.Y., and Chen, C.H., 2001. High-Mg potassic rocks from Taiwan: implications for the genesis of orogenic potassic lavas. *Lithos,* 59, p.153-170. DOI:10.1016/s0024-4937(01)00067-6

Condie, K.C., 2005. TTGs and Adakites: Are they both slab melts? *Lithos*, 80, p.33-44. DOI:10.1016/j.lithos.2003.11.001

Dempsey, S.R., 2013. *Geochemistry of volcanic rocks from the Sunda Arc*, Durham, Theses.

Dokuz, A., 2011. A slab detachment and delamination model for the generation of Carboniferous high-potassium I-type magmatism in the Eastern Pontides, NE Turkey: The Kose composite pluton. *Gondwana Research*, 19, p.926-944. DOI:10.1016/j.gr.2010.09.006.

Dostal, J., 2008. Series Igneous Rock Associations 10 (Komatiites). *Journal of the Geological Association of Canada*, 35 (1), p.21-31.

Edwards, C.M., Menzies, M.A., Thirlwall, M.F., Morris, J.D., Leeman, W.P., and Harmon, R.S., 1994. The transition to potassic alkaline volcanism in island arcs: The Ringgit–Beser complex, east Java, Indonesia. *Journal of Petrology*, 35, p.1557-1595. DOI:10.1093/petrology/35.6.1557

Foley, S.F., Venturelli, G., Green, D.H., and Toscani, L., 1987. The ultrapotassic rocks: characteristics, classification, and constraints for petrogenetic models. *Earth-Science*

Research, 24, p.81-134. DOI:10.1016/0012-8252(87)90001-8

Foley, S.F., 1992a. Petrological characterization of the source components of potassic magmas: geochemical and experimental constraints. *Lithos*, 28, p.187-204. DOI:10.1016/0024-4937(92)90006-k

Foley, S.F., 1992b. Vein-plus-wall-rock melting mechanisms in the lithosphere and the origin of potassic alkaline magmas. *Lithos*, 28, p.435-453. DOI:10.1016/0024-4937(92)90018-t

Frost, B.R. and Frost, C.D., 2008. A Geochemical Classification for Feldspathic Igneous Rocks. *Journal of Petrology*, 49 (11), p.1955-1969. DOI:10.1093/petrology/egn054

Gillespie, M.R. and Styles, M.T., 1999. *BGS Rock Classification Scheme*. 1. *Classification of igneous rocks*. British Geological Survey Research Report, 2nd edition.

Ghiorso, M.S. and Sack, R.O., 1995. Chemical Mass Transfer in Magmatic Processes. IV. A Revised and Internally Consistent Thermodynamic Model for the Interpolation and Extrapolation of Liquid-Solid Equilibria in Magmatic Systems at Elevated Temperatures and Pressures. *Contributions to Mineralogy and Petrology*, 119, p.197-212.

Godang, S., Fadlin, and Priadi, B., 2016. Geochemical Signatures of Potassic to Sodic Adang Volcanics, Western Sulawesi: Implications for Their Tectonic Setting and Origin. *Indonesian Journal on Geoscience*, 3 (3), p.195-214. DOI: 10.17014/ijog.3.3.195-214

Hatherton, T. and Dickinson, W.R., 1969. The relationship between andesitic volcanism and seismicity in Indonesia, the Lesser Antilles, and other island arcs. *Journal Geophysical Research,* 74, p.5301-5310.

Herzberg, C., 1995. Generation of plume magmas through time: an experimental approach. *Chemical Geology,* 126, p.1-16.

Herzberg, C., Asimow, P.D., Arndt, N., Niu, Y., Lesher, C.M., Fitton, J.G., and Saunders, A.D., 2007. Temperature in ambient mantle and plumes: Constraints from basalts, picrites, and komatiites. G*eochemistry, Geophysics, Geosystems*, 8, Q02006.

Hollocher, K., Robinson, P., Walsh, E., and Roberts, D., 2012. Geochemistry of amphibolite-facies volcanics and gabbros of the Støren Nappe in extensions west and southwest of Trondheim, Western Gneiss Region, Norway: a key to correlations and paleotectonic settings. *American Journal of Science*, 312, p.357-416. DOI: 10.2475/04.2012.01

Huang, Z.L., Liu, C.Q.., Yang, H.L., Xu, C., Han, R.S., Xiao, Y.H., Zhang B., and Li, W.B., 2002. The geochemistry of lamprophyres in the Laowangzhai gold deposits, Yunnan Province, China: Implications for its characteristics of source region. DOI:10.2343/geochemj.36.91

Jensen, L.S., 1976. *A New Cation Plot for Classifying Subalkalic Volcanic Rocks*,Miscellaneous Paper 66. Ministry of Natural Resources. 22pp.

Kelemen, P.B., 1995. Genesis of high Mg# andesites and the continental crust. *Contributions to Mineralogy and Petrology,* 120, p.1-19. DOI:10.1007/s004100050054

Kersting, A.B. and Arculus, R.J., 1994. Klyuchevskoy Volcano, Kamchatka, Russia: The Role of High-Flux Recharged, Tapped, and Fractionated Magma Chamber(s) in the Genesis of High-Al2O3 from High-MgO Basalt. *Journal of Petrology*, 35, p.1-41. DOI:10.1093/petrology/35.1.1

Kinzler, R.J., 1997. Melting of mantle peridotite at pressures approaching the spinel to garnet transition: Application to mid-ocean ridge basalt petrogenesis. *Journal of Geophysical Research*, 102, p.852-874. DOI:10.1029/96JB00988.

La Flèche, R., Camiré, G., Jenner, G.A., 1998. Geochemistry of post-Acadian, Carboniferous continental intraplate basalts from the Maritimes Basin, Magdalen islands, Québec, Canada. Chemical Geology 148, p.115–136.

Leeuwen, T. V. and Pieters, P.E., 2011. Mineral Deposits of Sulawesi. *Proceedings of the Sulawesi Mineral Resources*. Seminar MGEI-IAGI.

Le Maitre, R.M., Bateman, P., Dudek, A., Keller, J., Lameyre, J., Le Bas, M.J., Sabine, P.A., Schmid, R., Sorensen, H., Streckeisen, A., Woolley, A.R., and Zanettin, B., 1989. *A Classification of Igneous Rocks and Glossary of Terms*. Recommendations of the International Union of Geological Sciences Subcommission on the Systematics of Igneous Rocks. Blackwell Scientific Publications, Oxford, U.K. DOI: 10.1017/cbo9780511535581.005

Le Roex, A.P., Dick, H.J.B., Erlank, A.X, Reid, A.M., Frey, F.A., and Hart, S.R., 1983. Geochemistry, Mineralogy and Petrogenesis of Lavas Erupted along the Southwest Indian Ridge Between the Bouvet Triple Junction and 11 Degrees East. *Journal of Petrology*, 24 (3), p.267-318. DOI:10.1093/petrology/24.3.267

Luhr, J.F., 1997. Extensional tectonics and the diverse primitive volcanic rocks in the western Mexican volcanic belt. *Canadian Mineralogy*, 35, p.473-500.

MacLean, W.H. and Barrett, T.J., 1993. Lithogeochemical technique using immobile elements. *Journal of Geochemical Exploration,* 48 (2), p.109-133. DOI: 10.1016/0375-6742(93)90002-4

McDonough, W.F. and Sun, S.S., 1995. Composition of the Earth. *Chemical Geology*, 120, p.223-253.

Muller, D., Rock, N.M.S., and Groves, D.I., 1992. Geochemical discrimination between shoshonitic and potassic volcanic rocks in different tectonic settings: a pilot study. *Mineralogical Petrology*, 46, p.259-289. DOI:10.1007/bf01173568

Muller D. and Groves D.I., 1993. Direct and indirect associations between potassic igneous rocks, shoshonites and gold–copper deposits, *Ore Geology Reviews*, B (8), p.383-406. DOI:10.1016/0169-1368(93)90035-w

Muller, D. and Groves, D.I., 1993. Potassic Igneous Rocks and Associated Gold-copper Mineralization. *Lecture Notes in Earth Siences*, 56. *DOI:*10.1007/978-3-662-00920-8_10

Muller D. and Groves D.I., 2000. P*otassic igneous rocks and associated gold–copper mineralization*, 3rd ed. Springer, Berlin Heidelberg New York, 252pp. DOI:10.1007/978-3-642-59665-0_3

Nesbitt, H., and R. Wilson., 1992. Recent chemical weathering of basalts. *American Journal of Science*, 292, p.740-777. DOI:10.2475/ajs.292.10.740

Pearce, J.A., 2008. *Geochemical fingerprinting of oceanic basalts with applications to ophiolite classification and the search for Archean oceanic crust*. DOI:10.1016/j.lithos.2007.06.016

Peccerillo, A. and Taylor, S.R., 1976. Geochemistry of the Eocene calc-alkaline volcanic rocks from the Kastamonu area, northern Turkey. *Contributions to Mineralogy and Petrology*. p.63-81. DOI:10.1007/bf00384745

Peccerillo, A., 1999. Multiple mantle metasomatism in central–southern Italy: geochemical effects, timing and geodynamic implications. *Geology,* 27, p.315-318. DOI:10.1130/0091-7613(1999)027<0315:mmmics>2.3.co;2

Ratman, N. and Atmawinata, S., 1993. *Geological map of the Mamuju Quadrangle, Sulawesi, (scale 1:250.000)*. Geological Research and Development Centre, Bandung.

Rock, N.M.S., 1991. *Lamprophyres*. Springer Science+Business Media, LLC, 285pp.

Rogers, N.W., Hawkesworth, C.J., Mattey, D.P., and Harmon, R.S., 1987. Sediment subduction and the source of potassium in orogenic leucitites. *Geology*, 15, p.451-453. DOI:10.1130/0091-7613(1987)15<451:ssatso>2.0.co;2

Salters, V.J.M. and Stracke, A., 2004. Composition of the depleted mantle. *Geochemistry, Geophysics, Geosystems*, 5 (5), p.1-27. DOI:10.1029/2003GC000597.

Schilling, J.G., Zajac, M., Evans. R., Johnston. T., White. W., Devine, J.D. and Kingsley, R., 1983. Petrologic and geochemical variations along the Mid-Atlantic Ridge from 27°N to 73°N. *American Journal of Science*, 283, p.510-86.

Schmeling, H. and Arndt, N., 2017, Modelling komatiitic melt accumulation and segregation in the transition zone. *Earth and Planetary Science Letters*, 472, p. 95-106. DOI:10.1016/j.epsl.2017.05.021.

Sukadana, I.G., Harijoko, A., and Setijadji, L.D., 2015. Tectonic Setting of Adang Volcanic

Complex in Mamuju Region, West Sulawesi Province. *Eksplorium*, 36 (1), p.31-44. DOI:10.17146/eksplorium.2015.36.1.2769

Sun, S.Q., Zhang, C.J., and Huang, R.Q., 2006. The Tectonic Settings Discrimination of the Basalts in the Convergent Margin of Plate by Th, Nb and Zr. *Advances in Earth Science*, 21 (6), p.593-598. (in China Mandarin language).

Turner, S., Arnaud, N., Liu, J., Rogers, N., Hawkesworth, C., Harris, N., Kelley, S., Van Calsteren, P., and Deng, W., 1996. Postcollision, shoshonitic volcanism on the Tibetan, plateau: implications for convective thinning of the lithosphere and source of ocean island basalts. *Journal of Petrology*, 37, p.45-71. DOI:10.1093/petrology/37.1.45

Varne, R., 1985. Ancient subcontinental mantle: a source for K-rich orogenic volcanics. *Geology*, 13, p.405-408. DOI:10.1130/0091-7613(1985)13<405:asmasf>2.0.co;2

Wang, X.C., Li, X.H., Li, W.X., Li, and Zheng, X., 2007. Ca. 825 Ma komatiitic basalts in South China: First evidence for >1500°C mantle melts by a Rodinian mantle plume. p. 1103-1106. DOI:10.1130/g23878a.1

Woolley, A.R., Bergman, S.S., Edgar, A.D., Le Bas, M.J., Mitchell, R.H., and Rock, N.M.S., 1996. Classification of lamprophyres, lamproites, kimberlites, and the kalsilitic, melilitic, and leucitic rocks. *The Canadian Mineralogist*, 34, p.175-186.

Zhang, Y.X, 2014. Quantification of the elemental incompatibility sequence, and composition of the “superchondritic” mantle. *Chemical Geology,* 369, p.12-21. DOI:10.1016/j.chemgeo.2014.01.012